Plastic Deformation of Bicrystals composed of ⟨100⟩, ⟨111⟩, and Single Glide Oriented Aluminum Crystals

By

Sei MIURA* and Kazuo HAMASHIMA**

(Receiyed January 27, 1982)

Synopsis

When two crystal grains having large different deformation-modes are adjacent to each other, their compatibility at the boundary plane becomes extremely confused. Therefore, it is thought that such a grain boundary condition plays an important role on several phenomena of the materials containing it.

In this study, three kinds of bicrystals composed of two crystals within three kinds of single crystals (a common single crystal for single glide, a single crystal with ⟨100⟩ tensile orientation and a single crystal with ⟨111⟩ tensile orientation), are prepared and tested by tension.

The additional slips on {110} are activated, and the boundary strength is positive in the bicrystals composed of a crystal for single glide and a crystal with ⟨100⟩ tensile orientation.

In the bicrystals composed of a crystal for single glide and a crystal with ⟨111⟩ tensile orientation, a few clustered slips occur from the grain boundary in the grain with ⟨111⟩ tensile orientation. The boundary strength is negative.

Some micro-cracks are observed along the grain boundary of bicrystals composed of a crystal with ⟨100⟩ tensile orientation and a crystal with ⟨111⟩ tensile orientation. The boundary strength is found to be zero.

1. Introduction

How the grain boundary influences the mechanical properties of polycrystalline material can be understood fundamentally by studies using bicrystals having a single grain boundary. Such investigations have been performed by many researchers using bicrystal specimens of aluminum [1–8], β-Brass [9] and Fe-Si [10]. The effect of the grain boundary has been discussed from diverse viewpoints.

However, most of the bicrystals were isoaxial. Even if the bicrystal was non-isoaxial, the deformation modes of its component single crystals did not notably differ from one another. When the deformation modes of two grains opposite each other are markedly different, the microscopic imcompatibility is remarkable at

* Department of Engineering Science, Faculty of Engineering, Kyoto University, Kyoto, Japan.
** Department of Mechanical Engineering, Doshisha University, Kyoto, Japan.

the grain boundary plane separating those grains. Therefore, it is thought that this sort of grain boundary plays an important role in the diverse properties of polycrystalline materials (fatigue, fracture, etc.), but the effects of these grain boundaries on the plastic deformation of bicrystals have not been studied. This study is accordingly performed to fundamentally clarify their effects, using aluminum bicrystals.

In the present study, three types of non-isoaxial bicrystals: a bicrystal composed of a common single crystal for single glide and a single crystal with ⟨100⟩ tensile orientation (The quadruple slips occur immediately after yield and the cross slip can most easily occur), a bicrystal composed of a common single crystal for single glide and a single crystal with ⟨111⟩ tensile orientation (The triple slips occur immediately after yield and the occurrence of cross slip is most difficult.), and a bicrystal composed of a single crystal with ⟨100⟩ tensile orientation and a single crystal with ⟨111⟩ tensile orientation, were prepared. These bicrystals were tested in tension at room temperature so as to study in detail the effect of their grain boundaries on the flow stress, as well as the deformation mode of the bicrystals.

2. Experimental producedure

The material used in this experiment was 99.99 % pure aluminum. Plates of bicrystal, having orientation controlled by seeding, were grown by the Bridgman method in a vacuum. Specimens with a gauge dimension of $2\times5\times15\ mm^3$ were cut from the bicrystal plates by spark cutting, and then annealed at 823K for 3 hrs. All specimens were polished mechanically and electrolytically before a tensile test.

The orientation of these bicrystal specimens are shown in Fig. 1–(a) (b) (c). They are non-isoaxial and composed of two single crystals showing widely different deformation modes. The bicrystal shown in Fig. 1 (a) is composed of a common crystal for single glide and a crystal with ⟨100⟩ tensile orientation. The bicrystal shown in Fig. 1 (b) is composed of a common crystal for single glide and a crystal with ⟨111⟩ tensile orientation. The bicrystal shown in Fig. (c) is a combination of a crystal with ⟨100⟩ tensile orientation and a crystal with ⟨111⟩ tensile orientation. In this paper, the bicrystals shown in Fig. 1 (a)–(c) are named ⟨100⟩-Stage-I oriented bicrystal, ⟨111⟩-Stage I-oriented bicrystal and ⟨100⟩-⟨111⟩-oriented bicrystal respectively.

All bicrystal specimens have a grain boundary in the central section and parallel to the tensile direction in subsequent tensile testing. The accuracy with

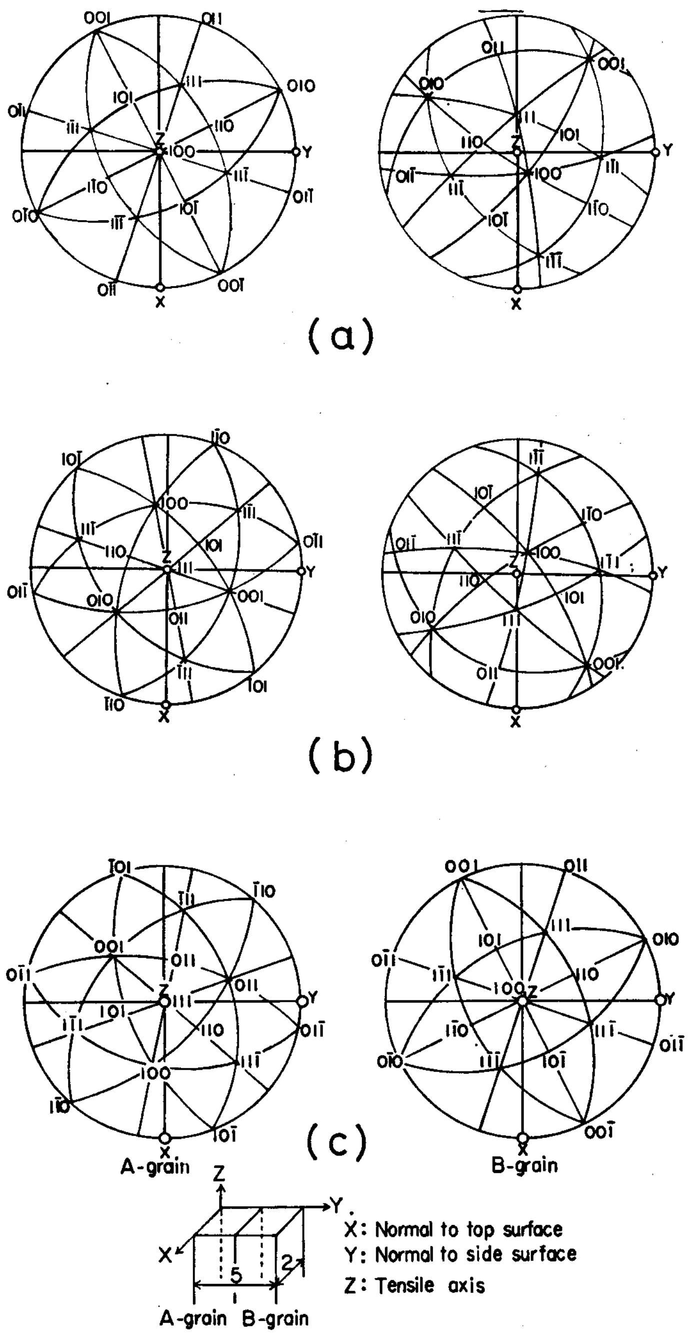

Fig. 1. The stereographic projection of the bicrystal, termed
(a) the ⟨100⟩-Stage I-oriented bicrystal.
(b) the ⟨111⟩-Stage I-oriented bicrystal.
(c) the ⟨100⟩-⟨111⟩-oriented bicrystal.

which the mis-orientations and boundary plane of the bicrystals could be controlled was within $\pm 0.5°$ and $\pm 1°$ respectively. Tensile tests were carried out with a strain rate of $4\times10^{-5}\text{sec}^{-1}$ at 293 ± 2K, using an Instron-type machine. A slip line observation was made at each stage of deformation.

3. Results and Discussion

3.1 Deformation mode of bicrystals

3.1.1 ⟨100⟩-Stage I-oriented bicrystal

Fig. 2 (a) and (b) show slip lines observed in the ⟨100⟩-Stage I-oriented bicrystal stretched by a 2.0 % and 10.5 % strain respectively. As the specimen surface was electrolytically polished several times during the experiment for the convenience of observation, a magnitude of strain at the observation at q %, and the last electrolytic polishing at p % are given in the figure as "p-q(%)".

The schmid factor (0.480) of the primary slip system in the B-grain (crystal for single glide) is somewhat larger than that (0.406) in the A-grain (crystal with ⟨100⟩ tensile orientation). Therefore, when this bicrystal is stretched, primary slips $(11\bar{1})$ and [101] of the B-grain are first activated. Subsequently, fine quadruple slips peculiar to a crystal with ⟨100⟩ tensile orientation begin to be observed in the A-grain, and conjugate slips of the B-grain begin to occur from about 1 % strain. (Fig. 2(a)). As the deformation proceeds, fine slip matching traces of the $(1\bar{1}0)$ plane are observed in the vicinity of the boundary of the A-grain. These slips originate from the boundary plane, and it is thought that they are induced by the primary slips of the B-grain. (Fig. 2(b))

Also, Fig. 2(b) shows that coarse slips accompanied by prominent cross slips (peculiar to a crystal with ⟨100⟩ tensile orientation) begin to occur in the A-grain

Table 1. N_{ij} value against each slip system due to the primary slip $(11\bar{1})$ [101] of B-grain, and m and m/m_0 values in A-grain of the ⟨100⟩-stage I-oriented bicrystal.

Slip plane	Slip direction	m	$\frac{m}{m_0}$	N_{ij} due to $(11\bar{1})$ [101]
(111)	$[1\bar{1}0]$	0.406	1	0.786
$(1\bar{1}1)$	$[10\bar{1}]$	0.406	1	0.441
	[110]	0.406	1	0.862
$(11\bar{1})$	$[1\bar{1}0]$	0.406	1	0.777
$(1\bar{1}\bar{1})$	[110]	0.406	1	0.751
$(1\bar{1}0)$	[110]	0.500	1.23	0.998

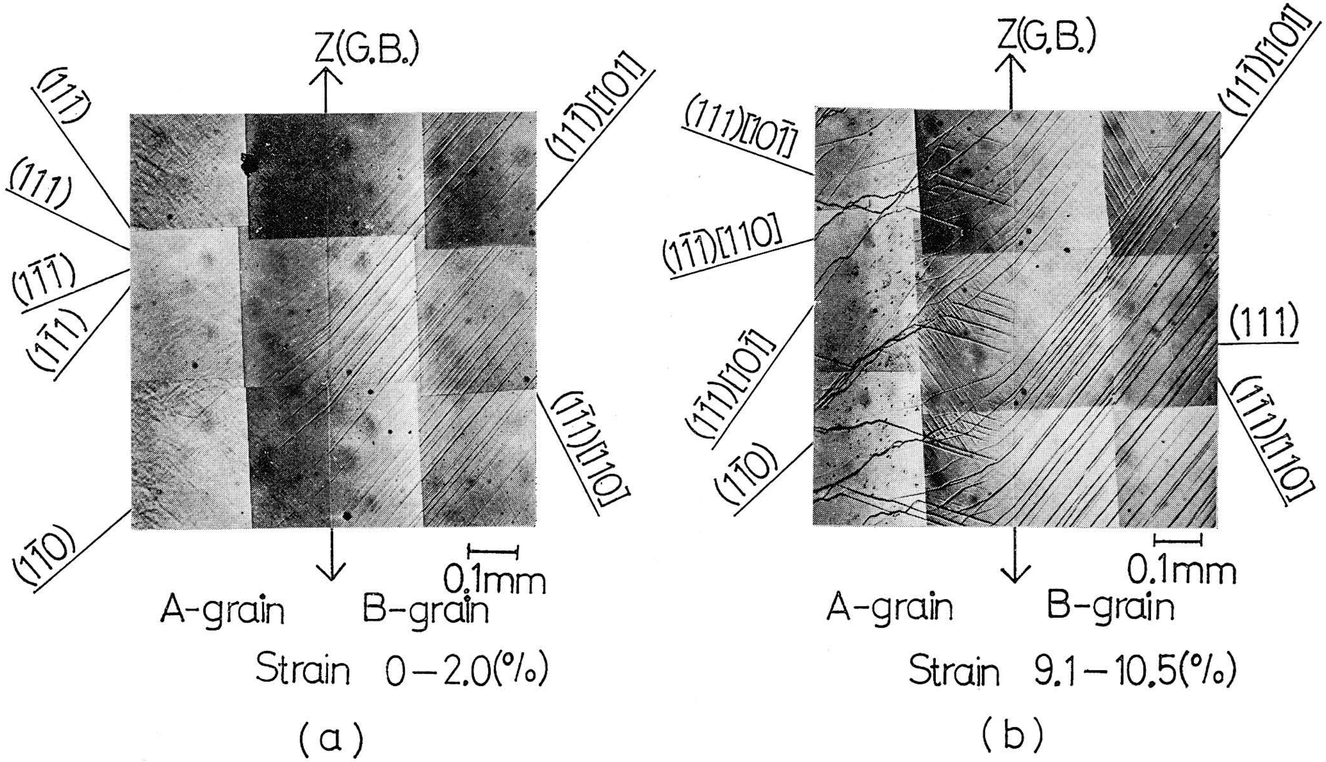

Fig. 2. Slip line observationn obtained in the ⟨100⟩-Stage I-oriented bicrystal stretched by (a) 2.0% strain, (b) 10.5 % strain.

at 3–4 % strain, and additional slips on the (111) plane occur in the vicinity of the boundary of the B-grain. Closer observation clarifies the fact that most of the primary slips of the B-grain reach the boundary plane, but few coarse slips of the A-grain arrive there. This discrepancy is thought to be caused for the following reasons. As the primary slips of the B-grain are activated prior to all the other slips, these slips are not influenced by the activation of other slips. On the other hand, the activation of the coarse slips of the A-grain is impeded by the stress field, due to piled-up dislocations on the primary slip system of the B-grain, in the vicinity of the boundary.

To determine the cause of these additional slips, the stress transmission factor N_{ij} [3], and the imcompatibility of the plastic strain are studied. At first, the N_{ij} value against each slip system in the A-grain due to the primary slip system $(11\bar{1})$ and [101] in the B-grain is calculated. Five systems having a large N_{ij} value are given in Table 1. The comparison of the Schmid factor of the primary slip system (m_0), and the Schmid factor of each slip system (m) is also tabulated in Table 1, since this comparison is very important when considering additional slips [7]. While Hosford et al. [12] and Saeki and Miura [11] reported that frequent cross slips between two {111} planes looked like slips on a {110} plane in a tensile test using an aluminum single crystal with ⟨100⟩ tensile orientation, the slip matching traces of the $(\bar{1}10)$ plane in this bicrystal are straighter and narrower, similar to slips on the {110} plane observed by Hazif et al. ([13, 14]) in an aluminum single crystal with ⟨100⟩ tensile orientation compressed at high temperature. The N_{ij} value against the $(1\bar{1}0)$ [110] slip system of the A-grain due to the primary slip system of the B-grain and the m/m_0 value of the $(1\bar{1}0)$ [110] slip system are 0.998 and 1.23 respectively. The N_{ij} and m/m_0 values are larger than those of all {111}⟨110⟩ slip systems in the A-grain. Therefore it is thought that the slip matching traces of $(1\bar{1}0)$ in this bicrystal are {110}-slips induced by the primary slips of the A-grain.

In the vicinity of the grain boundary at the large strain region, the coarse slips (111) and $[10\bar{1}]$ and the additional slips $(1\bar{1}0)$ and [110] are activated in the A-grain. The primary slips $(11\bar{1})$ and [101] and the additional slips on the (111) plane are activated in the B-grain. Three plastic strain compositions of these slip systems are listed in Table 2. Comparing the strain compositions of both grains, those of the former three slip systems (111) $[10\bar{1}]$ and $(1\bar{1}0)$ [110] in the A-grain, $(11\bar{1})$ [101] in the B-grain are rather imcompatible ($\varepsilon^A_{xx}=-0.581$ $\varepsilon^A_{zz}=0.906$ $\varepsilon^A_{xz}=-0.098$, $\varepsilon^B_{xx}=-0.446$ $\varepsilon^B_{zz}=0.434$ $\varepsilon^B_{xz}=0.173$). If it is assumed that the slip system of additional slips in the B-grain is (111) $[10\bar{1}]$, and the im-

Table 2. Plastic strain compositions of fore slip systems in the ⟨100⟩-stage *I*-orlented bicrystal.

Crystal	Slip plane	Slip derection	ε_{xx}	ε_{zz}	ε_{xz}
A	(111)	[10$\bar{1}$]	$-0.496S_i$	$0.406S_i$	$-0.098S_i$
	(1$\bar{1}$0)	[110]	$-0.085S_i$	$0.500S_i$	0
B	(111)	[10$\bar{1}$]	$-0.446S_i$	$0.434S_i$	$0.173S_i$
	(11$\bar{1}$)	[101]	$-0.088S_i$	$0.480S_i$	$-0.021S_i$

compatiblity of the strain compositions is somewhat reduced ($\varepsilon^B_{xx}=-0.534$ $\varepsilon^B_{zz}=0.914$ $\varepsilon^B_{xz}=0.152$). It can be concluded that these additional slips occur at (111) [10$\bar{1}$] to satisfy the compatibility of the plastic strain.

3.1.2 ⟨111⟩-Stage I-oriented bicrystal

When the ⟨111⟩-Stage I bicrystal is stretched, primary slips (11$\bar{1}$) and [101] of the B-grain (a single crystal for single glide) begin to occur immediately after yield, and fine triple slips, characteristic of a crystal with a ⟨111⟩ tensile orientation, and a few clustered slips are subsequently activated in the A-grain (a single crystal with a ⟨111⟩ tensile orientation). The clustered slips occur from the grain boundary plane. (Fig. 3 (a) (b)). As the plastic strain increases, the conjugate slips (1$\bar{1}$1) and [101] and additional slips matching the (111) plane in the vicinity of the grain boundary are observed in the B-grain. In the A-grain, only triple slips occur at the latter stage of deformation, and the clustered slips do not occur except for the first stage of deformation. (Fig. 3 (b)).

The clustered slips, which were due to a slight difference in the resolved shear stress among the active slip systems, were observed in a single crystal with tensile orientation inclining a few degrees to ⟨111⟩ by the present authors [15]. The resolved shear stress of six active slip systems in this bicrystal are equal, but it is thought that the additional stress caused by piled-up dislocations on the primary slip system of the B-grain induces the clustered slips of the A-grain.

The N_{ij} values against all possible slip systems in the A-grain due to the primary slip system of the B-grain and m/m_0 are given in Table 3. The slip plane of the slip system having the maximum N_{ij} (11$\bar{1}$) and [011], agrees with the slip plane of the clustered slips in this bicrystal. Consequently, it is concluded that these coarse slips are induced by the primary slips of the B-grain. The reason for the absence of clustered slips at a large strain is similar to that explained in a previous paper [15].

At a large strain, the additional slips matching (111) plane occur in the vicinity of the B-grain, although only fine triple slips occur in the A-grain. It is

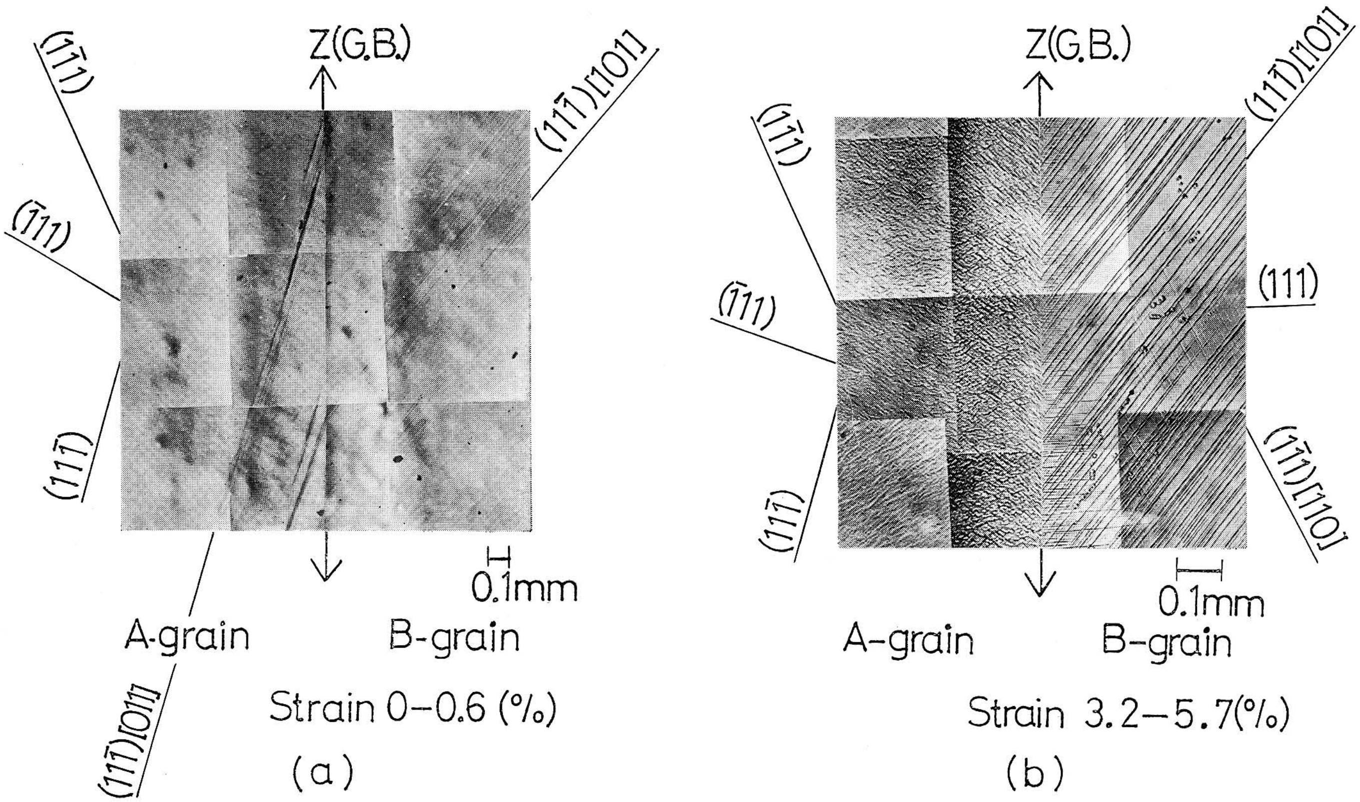

Fig. 3. Slip line observation obtained in the ⟨111⟩-Stage I-oriented bicrystal stretched by (a) 0.6% strain, (b) 5.7% strain.

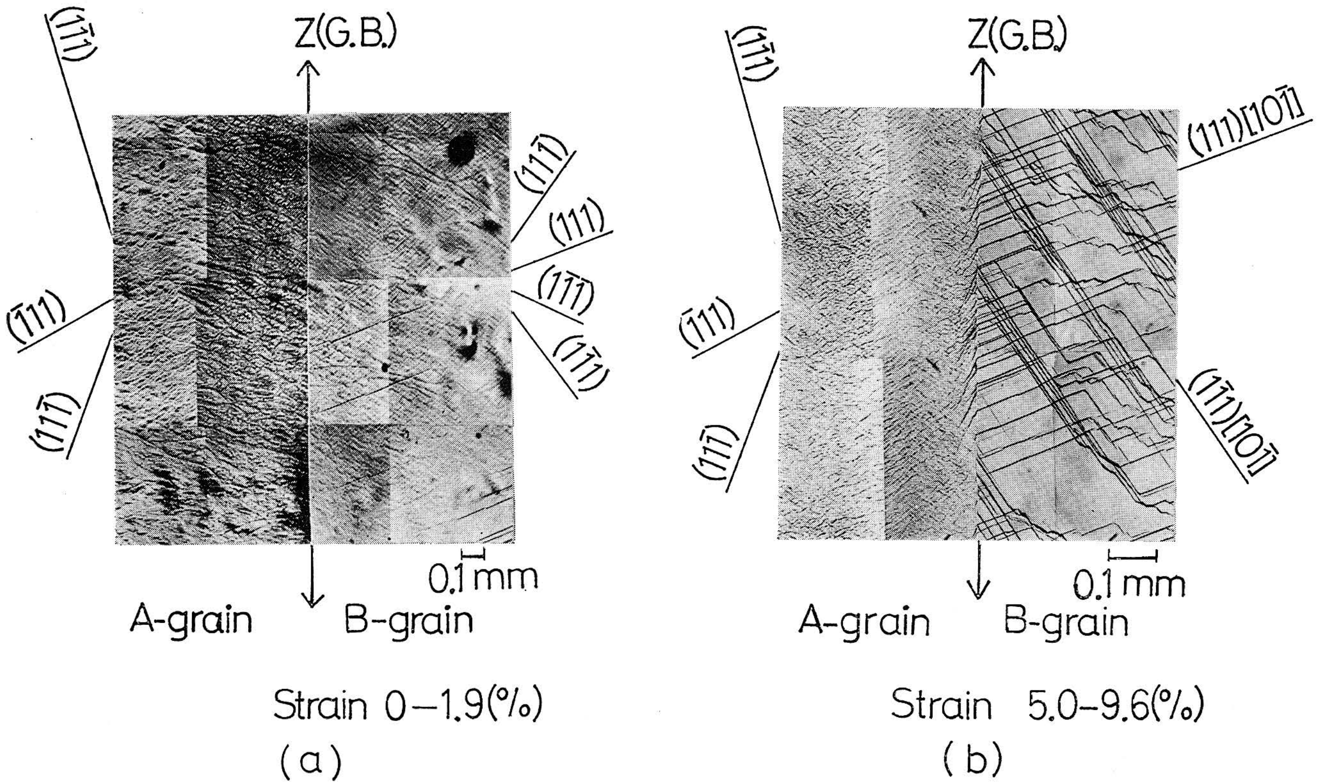

Fig. 4. Slip line observation obtained in the ⟨100⟩-⟨111⟩-oriented bicrystal stretched by (a) 1.9% strain, (b) 9.6% strain.

Table 3. N_{ij} value against each slip system due to the primary slip $(11\bar{1})$ [101] of *B*-grain, and *m* and m/m_0 values in *A*-grain the ⟨111⟩-stage *I*-oriented bicrystal.

Sllip plane	Slip direction	m	$\frac{m}{m_0}$	N_{ij} due to $(11\bar{1})$ [101]
$(1\bar{1}1)$	[110]	0.264	1	0.438
	[011]	0.264	1	0.067
$(11\bar{1})$	[011]	0.264	1	0.670
	[101]	0.264	1	0.588
$(\bar{1}11)$	[110]	0.264	1	0.552
	[101]	0.264	1	0.055

thought that the additional stress against slips of the B-grain due to such fine triple slips is not enough to induce slips. Therefore, these additional slips are thought to be activated so as to satisfy the compatibility of the plastic strain. However, the three plastic-strain-compositions of both grains cannot be compared, as a slip system of individual fine slips cannot be determined.

3.1.3 ⟨100⟩-⟨111⟩-oriented bicrystal

When the ⟨100⟩-⟨111⟩-oriented bicrystal is stretched, fine quadruple slips in the B-grain (single crystal with ⟨100⟩ tensile orientation) and fine triple slips in the A-grain (single crystal ⟨111⟩ tensile orientation) are activated immediately after yield. These slips have no influence on each other even in the vicinity of the grain boundary. (Fig. 4 (a))

Coarse slips accompanied by prominent cross slips begin to occur at about 1.5 % strain in the B-grain, and these slips propagate from end to end of the B-grain as in the proceeding deformation. (Fig. 4(b)) Careful observation at the large strain shows that the coarse slip, $(111)[10\bar{1}]$, of the B-grain induces additional slip matching traces of $(11\bar{1})$ in the vicinity of the grain boundary in the A-grain. The coarse slip, $(1\bar{1}1)[10\bar{1}]$ of the B-grain creates a micro-crack along the grain boundary. (Fig. 5)

It is thought that this micro-crack is due to the extreme difference on the strain-energy of the individual slips occurring at both sides of the grain boundary plane. To clarify why two sorts of coarse slips on different slip systems have different affects at the grain boundary, the two following considerations are pursued.

The N_{ij} value against each slip system in the A-grain due to (111) $[10\bar{1}]$ and $(1\bar{1}1)$ $[10\bar{1}]$ in the B-grain, and the m/m_0 value are tabulated in Table 4(a) (b). It is thought that additional slip matching traces of $(11\bar{1})$ are slips of $(11\bar{1})$ [011], but no factors of any creation of micro-cracks are found from Table 4 (a) (b).

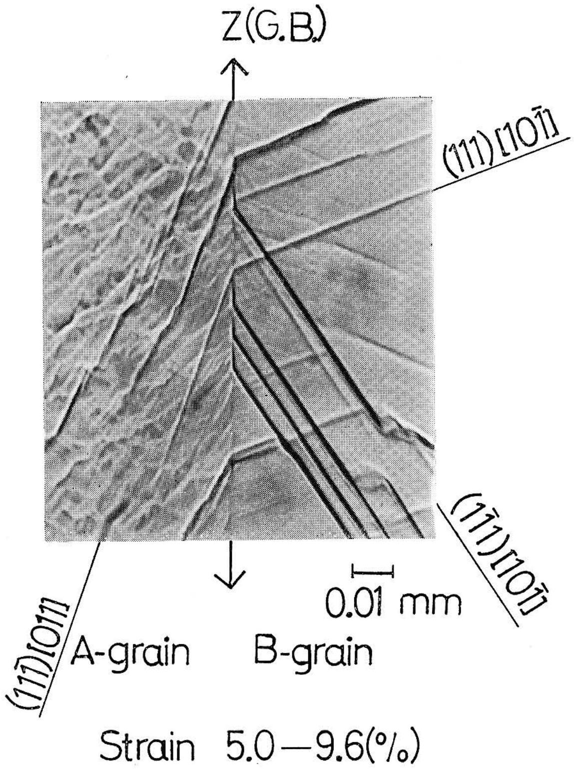

Fig. 5. The additional slips and short crevices in the vicinity of grain boundary of the ⟨100⟩-⟨111⟩-oriented bicrystal, strectched by 9.6% strain.

Table 4. The values of m, m/m_0 and N_{ij} against each slip system due to
(a) the coarse slip: (111) [10$\bar{1}$] of B-grain,
(b) the coarse slip: (1$\bar{1}$1) [10$\bar{1}$] of B-grain,
in A-grain of the ⟨100⟩-⟨111⟩-oriented bicrystal.

(a)

Slip plane	Slip direction	m	$\frac{m}{m_0}$	N_{ij} due to (111) [10$\bar{1}$]
(1$\bar{1}$1)	[110]	0.264	1	0.224
	[011]	0.264	1	0.064
(11$\bar{1}$)	[011]	0.264	1	0.767
	[101]	0.264	1	0.108
($\bar{1}$11)	[110]	0.264	1	0.828
	[101]	0.264	1	0.436

(b)

Slip plane	Slip direction	m	$\frac{m}{m_0}$	N_{ij} due to (1$\bar{1}$1) [10$\bar{1}$]
(1$\bar{1}$1)	[110]	0.264	1	0.797
	[011]	0.264	1	0.270
(11$\bar{1}$)	[011]	0.264	1	0.321
	[101]	0.264	1	0.446
($\bar{1}$11)	[110]	0.264	1	0.244
	[101]	0.264	1	0.089

Moreover, it cannot be thought that the imcompatibility of the plastic strain causes a nucleation of short cracks. Therefore, it seems that the difference of operation by both coarse slips in the vicinity of the grain boundary is due to the reaction of an active dislocation and a boundary dislocation. An analysis using such conditions is our future project.

3.2 Deformation mode and Boundary strength

The stress-strain curves of three kinds of bicrystals, their component single crystals and their provisional bicrystals are shown in Fig. 6. In Fig. 6, the stress

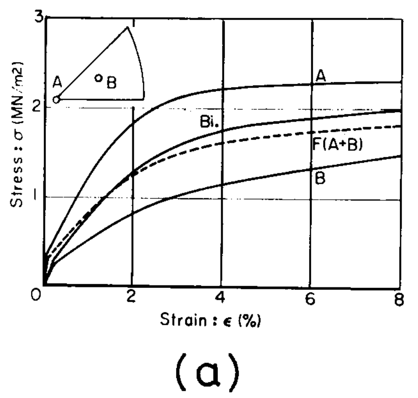

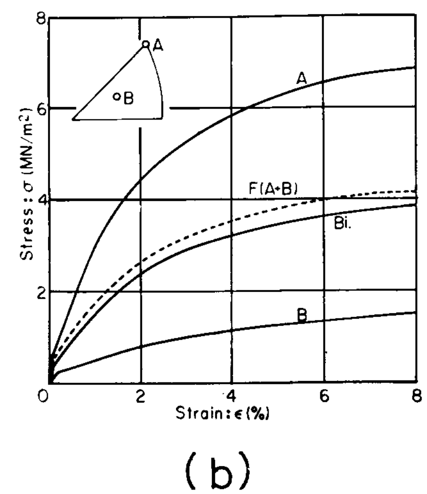

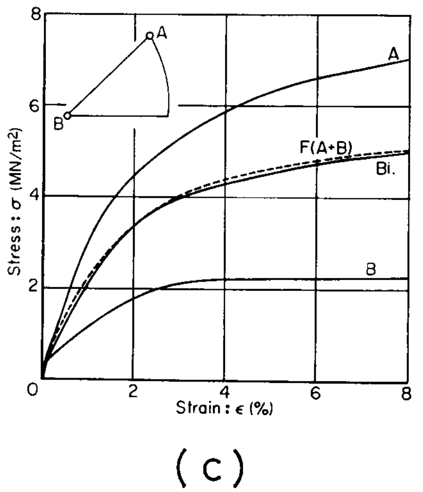

Fig. 6. The stress-strain curves of
(a) the ⟨100⟩-Stage I-oriented bicrystal,
(b) the ⟨111⟩-Stage I-oriented bicrystal,
(c) the ⟨100⟩-⟨111⟩-oriented bicrystal,
their component single crystals and their provisional bicrystals.

of the provisional bicrystal $F(A+B)$ is given by

$$F(A+B) = \frac{A_a}{A}\cdot\sigma_{SA}+\frac{A_b}{A}\cdot\sigma_{SB} \tag{1}$$

where A is the cross-sectional area of the bicrystal, A_a and A_b are the cross sectional areas of the component single crystals A and B respectively, and σ_A and σ_B are the flow stress of the component single crystals A and B. Futhermore, the boundary strength of the bicrystal is obtained as

$$\Delta\sigma = \sigma_{Bi} - F(A+B) \tag{2}$$

where σ_{Bi} is the flow stress of the bicrystal. The relation of the boundary strength and the plastic strain is shown in Fig. 7. The boundary strength of the ⟨100⟩-

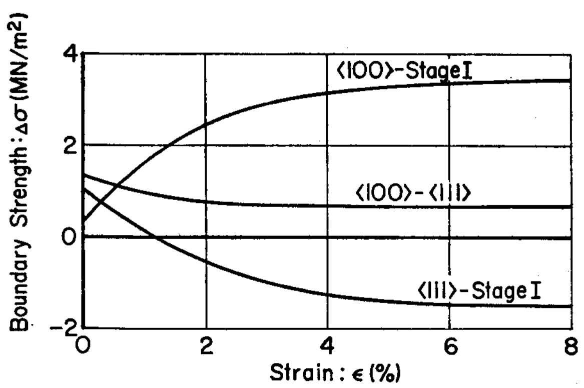

Fig. 7. The effect of plastic strain on the boundary strength of the respective bicrystals.

Stage I-oriented bicrystal increases rapidly at 0–3 % strain, but has almost no increase thereafter. The boundary strength of the ⟨111⟩-Stage I-oriented bicrystal has a negative value, but its value multiplies rapidly at 0–3 % strain and is also almost constant thereafter. The boundary strength of the ⟨100⟩-⟨111⟩-oriented bicrystal is constant (0.7 MN/m^2), having nothing to do with strain. As this constant value is small enought to ignore (about 2 % of the flow stress of the bicrystal at 2 % strain), it is thought that the boundary strength of this bicrystal is almost zero.

Many researchers have confirmed that the boundary strength is positive, with a few exceptions [5] [6], owing to the interaction of additional slips, clustereds slips or a back-stress from boundary. This is the case also in this study, as the flow stress of the ⟨100⟩-Stage I-oriented bicrystal is added by the additional slips $(1\bar{1}\bar{1})[110]$ induced in the vicinity of the grain boundary immediately after the yield. Its boundary strength is positive.

The clustered slips occur in the grain with a ⟨111⟩ tensile orientation of the ⟨111⟩-Stage I-oriented bicrystal at the initial stage of the plastic deformation. (See 3.1.2.) The flow stress of a single crystal, which has a tensile orientation inclining a few degrees to ⟨111⟩, falls considerably lower than that of a crystal with a ⟨111⟩ tensile orientation (about 15 %), due to the clustered slips.

Also in this bicrystal, as the clustered slips are induced by the primary slips of neighboring grain in the grain with a ⟨111⟩ tensile orientation, the flow stress of this grain is lowered. As a consequence, the flow stress of this bicrystal is lowered by the activation of these clustered slips, and this bicrystal has a negative boundary strength.

Davis et al. [2] and this author et al. [8] showed that the flow stress of an-aluminum isoaxial bicrystal having a multiple-slip-orientation was equal to that of its component single crystals. In such a bicrystal, as the work-hardening due to interactions of active slips in an individual grain is extremely large, the interaction of the grain boundary and active slips hardly contributes to an increase of the flow stress. The ⟨100⟩-⟨111⟩-oriented bicrystal is not isoaxial, but a pair of single crystals with a multiple-slip-orientation. Therefore, no effect of the grain boundary on the flow stress is observed.

4. Summary

The effects of the grain boundary on the plastic properties of a ⟨100⟩-Stage I-oriented bicrystal, a ⟨111⟩-Stage I-oriented bicrystal and a ⟨100⟩-⟨111⟩-oriented bicrystal were studied.

In the ⟨100⟩-Stage I-oriented bicrystal, additional slips having a {110} slip plane are induced in the grain with a ⟨100⟩ tensile orientation from the initial stage of deformation. The boundary strength of this bicrystal is positive, due to the occurence of these additional slips.

The flow stress of the ⟨111⟩-Stage I-oriented bicrystal is lowered, because the clustered slips are activated by primary slips of the grain for the single glide in the grain with a ⟨111⟩ tensile orientation. The boundary strength is negative as a consequence.

The deformation modes of both composing grains are not mutually influenced in the ⟨100⟩-⟨111⟩-oriented bicrystal, and the boundary strength of this bicrystal is zero in appearance. It is found that the coarse slip of a specific slip system in the grain with a ⟨100⟩ tensil orientation forms micro-cracks on the grain boundary plane.

The authors wish to thank the Sumitomo Light Metal Industries Ltd., Japan, for a generous supply of materials. Thanks are also due to Messrs. N. Sugiura and M. Nakano, students of Doshisha Univ., for their help in the course of the experimental work. Finally, the authors acknowledge with gratitude the financial support given by the Light Metals Educational Foundation of Japan.

References

1) R. Clark and B. Chalmers, Acta Met., **2**, 80 (1954).
2) R.S. Davis, R.L. Fleischer, J.D. Livingston and B. Chalmers, Trans. AIME **209**, 136 (1957).
3) J.D. Livingston and B. Chalmers, Acta Met., **5**, 322 (1957).
4) J.J. Hauser and B. Chalmers, Acta Met., **9**, 802 (1961).
5) T. Inoko, K. Akizono and G. Mima, J. Japan Inst. Metals, **36**, 373, 380 (1972).
6) O. Izumi and T. Takasugi, Z. Mettallkde, **65**, 542 (1974).
7) Y. Saeki and S. Miura, Mechanical Behavior of Materials. (Proc. 1974 Symp. of Mech. Behavior of Materials, Kyoto, 1974, The Society of Materials Science, Japan), Vol. II p. 11 (1974).
8) S. Miura and Y. Saeki, Acta Met., **26**, 93 (1978).
9) Y. Chuang and H. Margolin, Metall. Trans. **4**, 1905 (1973).
10) R.E. Hook and J.P. Hirth, Acta Met., **15** 535, 1099 (1967).
11) Y. Saeki and S. Miura, Trans. JIM, **18** 843 (1977).
12) W.F. Hosford, Jr., R.L. Fleischer, and W.F. Backofen, Acta Met., **8** 187 (1960).
13) R.L. Hazif, P. Dorizzi, and J.P. Poirier, Acta Met., **21** 903 (1973).
14) R.L. Hazif and J.P. Poirier, Acta Met., **23**, 865 (1975).
15) S. Miura and K. Hamashima, J. Soc. Mat. Sci. Japan **27**, 1146 (1978).